DALTON

The crystal structures of $[NMe_4][(Me_2AsO_2)\{MoO(O_2)_2\}_2]$, $[NMe_4][(Ph_2PO_2)\{MoO(O_2)_2\}_2]$, $[NBu^n_4][(Ph_2PO_2)\{WO(O_2)_2\}_2]$ and $[NH_4][(Ph_2PO_2)\{MoO(O_2)_2(H_2O)\}]$ and their use as catalytic oxidants †

N. Melanie Gresley, William P. Griffith,* Bernardeta C. Parkin, Andrew J. P. White and David J. Williams *

Inorganic and Chemical Crystallographic Research Laboratories, Department of Chemistry, Imperial College of Science, Technology and Medicine, London SW7 2AY, UK

The new heteropolyperoxometalate compounds $[NMe_4][(Me_2AsO_2)\{MoO(O_2)_2\}_2]$ **1**, $[NMe_4][(Ph_2PO_2)\{MoO(O_2)_2\}_2]$ **2**, $[NBu^n_4][(Ph_2PO_2)\{WO(O_2)_2\}_2]$ **3** and $[NH_4][(Ph_2PO_2)\{MoO(O_2)_2(H_2O)\}]$ **4** have been isolated and their crystal structures determined. Compounds **1**–**3** are dinuclear, whilst compound **4** is mononuclear; in all four structures the metal centre(s) have essentially identical pentagonal-bipyramidal co-ordination geometries with a weak axial ligand *trans* to an oxo group. The utility of **3** as a catalyst for the oxidation of alkenes, alcohols and tertiary amines with hydrogen peroxide as cooxidant has been studied.

Catalysis of the homogeneous oxidation of organic substrates by environmentally acceptable reagents such as hydrogen peroxide is of current interest.[1–5] In this series of papers[1,2,6] we have explored the use of molybdenum and, in particular, tungsten iso- and hetero-polyperoxo complexes as catalysts for organic oxidations with hydrogen peroxide as cooxidant. A prerequisite for such oxidations to be effective appears to be the presence of an η^2,η^1-peroxo moiety in which one of the oxygen atoms of a peroxo ligand, side-bonded to a metal atom, forms a weak bond to an adjacent metal atom. The presence of such bonds was first demonstrated in 'Venturello's compound', $[N(C_6H_{13})_4]_3[PO_4\{WO(O_2)_2\}_4]$.[3] This will, with hydrogen peroxide as cooxidant, catalyse the epoxidation of alkenes,[2,3] the conversion of tertiary amines to *N*-oxides,[6] internal alkynes to the corresponding α,β-epoxy ketones,[7,8] allenes to α-alkoxy or α-hydroxy ketones,[9] alkenes to carboxylic acids,[10] amines to oximes and nitrones,[11] anilines to azoxynitroso- and nitro-benzenes[12] and sulfides to sulfoxides and sulfones.[13]

We have been investigating the use of organo-phosphorus and -arsenic ligands in such heteropolyperoxo species with the aim of facilitating their attachment to solid-state supports. Here, we report the crystal structures of three new complexes containing η^2,η^1-linkages, $[NMe_4][(Me_2AsO_2)\{MoO(O_2)_2\}_2]$ **1**, $[NMe_4][(Ph_2PO_2)\{MoO(O_2)_2\}_2]$ **2** and $[NBu^n_4][(Ph_2PO_2)\{WO(O_2)_2\}_2]$ **3**, and also the structure of a related mononuclear species $[NH_4][(Ph_2PO_2)\{MoO(O_2)(H_2O)\}]$ **4** which contains only η^2-peroxo groups. Although we have previously reported[2] the existence of salts of $[AsO_4\{WO(O_2)_2\}_4]^{3-}$, complex **1** is the first structurally characterised example of an arsenic-containing polyperoxometalate. In line with our earlier observations,[1,2,6] we find that the tungsten-containing complex **3** is effective for alkene epoxidation, alcohol oxidation and the oxidation of tertiary amines, all with hydrogen peroxide as cooxidant.

Results and Discussion

Preparations and crystallography

Preparation and crystal structure of complex 1. The complex was isolated as a bright yellow crystalline solid by reacting $MoO_3{\cdot}H_2O$, H_2O_2, $Na[Me_2AsO_2]$ and $[NMe_4]Cl$ in a water–ethanol mixture followed by cooling at 0 °C for 3 d. No tungsten analogue could be obtained under similar reaction conditions using $WO_3{\cdot}H_2O$.

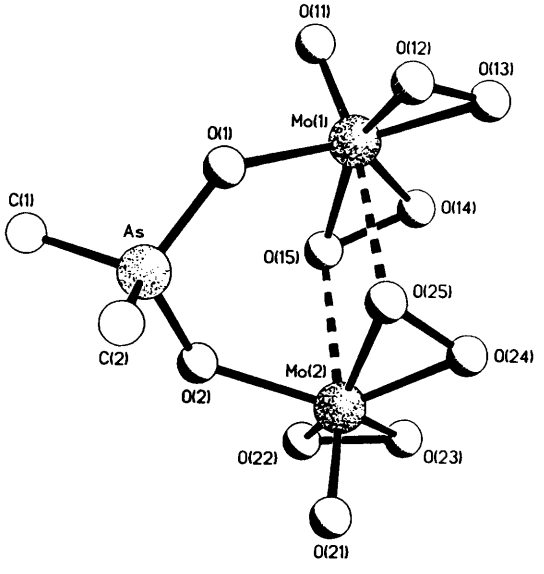

Fig. 1 Structure of the anion in complex **1**

The crystal structure of complex **1**, Fig. 1, shows the complex to have non-crystallographic C_2 symmetry about an axis passing through the arsenic atom and bisecting the vector linking the two molybdenum centres. Both of the metal ions have distorted pentagonal-bipyramidal geometries, a least-squares fit of which had a root mean square (r.m.s.) deviation of 0.02 Å for the co-ordinated atoms. The primary axial position on each metal centre carries an oxo ligand. Four of the equatorial sites around each of the molybdenum atoms are occupied by two bidentate peroxo groups, the fifth site in each case being filled by an oxygen atom from the dimethylarsinate ligand. One of the peroxo groups on each metal ion is of the non-bridging η^2-type, whereas the other [O(14)–O(15), O(24)–O(25)] is involved in bridging between Mo(1) and Mo(2) in an η^2,η^1 fashion. The consequence of these secondary axial interactions (depicted by broken bonds in Fig. 1) is not a lengthening of either peroxide bond (which remain at *ca.* 1.47 Å with an angle subtended at the 'parent' molybdenum atom of around 44°) but

† Studies on Polyoxo- and Polyperoxo-metalates. Part 4.[1]

Table 1 Selected bond lengths (Å) and angles (°) for complexes **1**–**4**

	1[a]	**2**[b]	**3**[c]	**4**[b]
X–O(1)	1.700(4)	1.525(2)	1.501(9)	1.536(2)
X–O(2)	1.691(4)	1.524(2)	1.502(9)	1.488(2)
X–C	1.874(6), 1.901(6)	1.781(2), 1.776(2)	1.763(10), 1.769(13)	*d*
M(1)–O(1)	2.007(4)	2.043(2)	1.925(9)	2.016(2)
M(2)–O(2)	2.020(4)	2.029(2)	2.036(9)	—
M(1)–O(11)	1.671(4)	1.668(2)	*d*	1.670(2)
M(1)–O(12)	1.923(4)	1.916(2)	*d*	1.936(2)
M(1)–O(13)	1.928(4)	1.910(3)	*d*	1.930(2)
M(1)–O(14)	1.920(4)	1.922(2)	*d*	1.936(2)
M(1)–O(15)	1.997(4)	1.981(2)	*d*	1.947(2)
M(1)–O(25)	2.426(4)	2.478(2)	*d*	2.368(2)[e]
M(2)–O(21)	1.653(5)	1.657(2)	*d*	—
M(2)–O(22)	1.928(4)	1.920(3)	*d*	—
M(2)–O(23)	1.915(4)	1.914(3)	*d*	—
M(2)–O(24)	1.922(4)	1.919(2)	*d*	—
M(2)–O(25)	2.005(4)	1.977(2)	*d*	—
M(2)–O(15)	2.439(4)	2.534(2)	*d*	—
O(12)–O(13)	1.457(7)	1.468(4)	*d*	1.469(3)
O(14)–O(15)	1.458(5)	1.468(3)	*d*	1.474(3)
O(22)–O(23)	1.480(6)	1.463(4)	*d*	—
O(24)–O(25)	1.466(6)	1.470(3)	*d*	—
M(1)–O(1)–X	132.6(2)	133.58(13)	140.3(7)	140.61(13)
M(2)–O(2)–X	129.4(2)	137.06(13)	136.9(5)	—
O(12)–M(1)–O(13)	44.5(2)	45.11(12)	*d*	44.65(10)
O(14)–M(1)–O(15)	43.7(2)	44.15(10)	*d*	44.62(9)
O(22)–M(2)–O(23)	45.3(2)	44.87(12)	*d*	—
O(24)–M(2)–O(25)	43.8(2)	44.32(10)	*d*	—
O(11)–M(1)–O(25)	170.7(2)	170.49(11)	*d*	179.93(10)
O(21)–M(2)–O(15)	168.1(2)	171.65(11)	*d*	—

[a] M = Mo, X = As. [b] M = Mo, X = P. [c] M = W, X = P. Values for major occupancy orientation only. [d] Values unreliable due to disorder (see text). [e] Aqua ligand.

an increase in the bond length to the parent molybdenum centres of the bridging oxygen atoms O(15) and O(25) [Mo(1)–O(14) 1.920(4), Mo(1)–O(15) 1.997(4), Mo(2)–O(24) 1.922(4) and Mo(2)–O(25) 2.005(4) Å]. The bridging bond lengths to the second metal atoms [O(15)–Mo(2) 2.439(4) and O(25)–Mo(1) 2.426(4) Å] are comparable with those found in $[NMe_4]_2[(PhPO_3)\{MoO(O_2)_2(H_2O)\}\{MoO(O_2)_2\}_2]$,[1] $[N(C_6H_{13})_4]_3[PO_4\{WO(O_2)_2\}_4]$[3] and $[NBu^n_4]_2[\{PO_3(OH)\}\{WO(O_2)_2\}_2]$.[14] The angles between the peroxo groups are *ca.* 127° whilst those between the peroxo groups and the bridging arsinate donor atoms are in the range 108 to 112°.* In each case, the molybdenum centres are displaced towards the oxo ligand relative to the plane of the five equatorial oxygen atoms by 0.40 and 0.41 Å for Mo(1) and Mo(2) respectively.† The angles between the axial ligands are 171° [for Mo(1)] and 168° [for Mo(2)].

The geometry at arsenic is tetrahedral, with angles in the range 107–115° with virtually identical arsenic–oxygen bond lengths [As–O(1) 1.700(4) and As–O(2) 1.691(4) Å]. There are no significant intermolecular interactions other than normal van der Waals. A comparison of selected bond lengths and angles for this and the structures of complexes **2**, **3** and **4** is given in Table 1.

Preparation and crystal structure of complex 2. The complex was isolated as a bright yellow crystalline solid by reacting $MoO_3{\cdot}H_2O$, H_2O_2, $Ph_2PO(OH)$ and $[NMe_4]Cl$ in a water–ethanol mixture followed by cooling at 0 °C for 3 d. A tetrabutylammonium salt was also synthesised.

The X-ray analysis of complex **2**, Fig. 2, reveals a structure

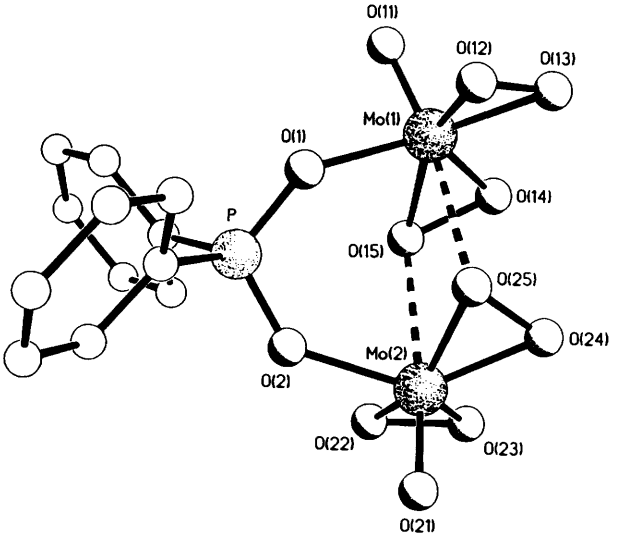

Fig. 2 Structure of the anion in complex **2**

that is geometrically virtually identical with that of **1**, but with the dimethylarsinate unit being replaced by a diphenylphosphinate. Both molybdenum centres have pentagonal-bipyramidal geometries, a least-squares fit of which, compared with that observed in **1**, has a r.m.s. deviation of only 0.03 Å. In common with **1**, there are both η^2- and η^2,η^1-peroxo groups on each metal ion, the latter [O(14)–O(15) and O(24)–O(25)] exhibiting a lengthening of the parent Mo–O bond in a fashion analogous to **1** [Mo(1)–O(14) 1.922(2), Mo(1)–O(15) 1.981(2), Mo(2)–O(24) 1.919(2) and Mo(2)–O(25) 1.977(2) Å], see Table 1.

The geometry at phosphorus shows only small deviations from tetrahedral, with angles in the range 106–114°; the two

* Considering each peroxo group as a unidentate ligand associated with a trigonal-bipyramidal geometry around each metal centre.

† The five equatorial co-ordinated oxygen atoms are coplanar to within 0.11 Å for both Mo(1) and Mo(2).

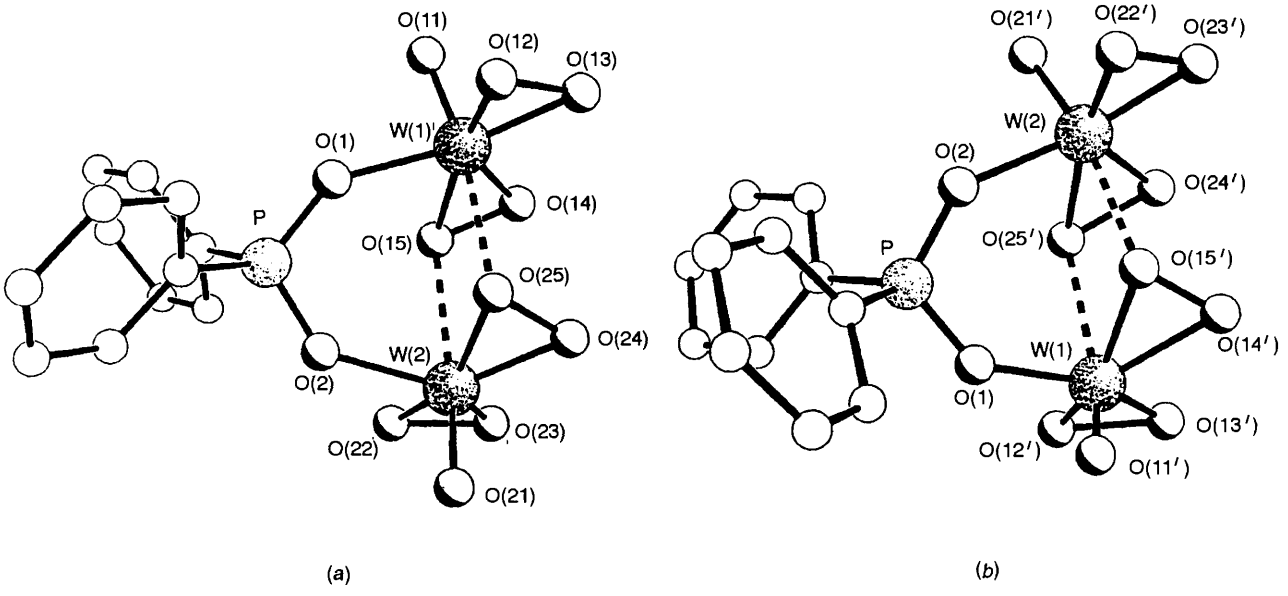

Fig. 3 Structures of (*a*) the major occupancy conformer and (*b*) the enantiomer of the minor occupancy conformer of the anion in complex **3**

P–O distances are the same [P–O(1) 1.525(2) and P–O(2) 1.524(2) Å]. Again, there are no significant intermolecular interactions.

Preparation and crystal structure of complex 3. The complex was isolated as a colourless crystalline solid by reacting $WO_3 \cdot H_2O$, H_2O_2, $Ph_2PO(OH)$ and $[NBu^n_4]Cl$ in a water–ethanol mixture followed by cooling at 0 °C for 2 months. Despite many attempts with other cations, only the tetrabutylammonium salt could be isolated.

The X-ray analysis of complex **3** reveals a disordered structure, the major occupancy component of which has an overall geometry [Fig. 3(*a*)] essentially the same as that of the molybdenum analogue **2**. The minor occupancy conformer, which is present with 45% occupancy, has a geometry for the tungsten co-ordination spheres which is virtually unchanged. Between both conformers, the two tungsten centres, the phosphorus and the bridging W–O–P oxygen atoms are overlaid. but the peroxo and oxo ligands are enantiomeric with respect to the major occupancy conformation. The equivalence of these two conformers can be visualised by taking the enantiomer of the minor occupancy conformer, Fig. 3(*b*), the only difference between the two geometries then being a reversal (or mirroring) of the pitch of the two phenyl rings. This disorder precludes discussion of the fine detail of the co-ordination geometries, and only the pertinent bond lengths and angles are summarised in Table 1. Despite this disorder, the η^2,η^1-linked pentagonal-bipyramidal co-ordinations are definitive. There are, again, no significant intermolecular interactions.

Preparation and crystal structure of complex 4. The complex was isolated as a bright yellow crystalline solid by reacting $MoO_3 \cdot H_2O$, H_2O_2, $Ph_2PO(OH)$ and NH_4Cl in a water–ethanol mixture followed by cooling at 0 °C for 3 d. Despite many attempts with other cations, only the ammonium salt could be isolated. Reactions were attempted under similar conditions using $WO_3 \cdot H_2O$ in place of $MoO_3 \cdot H_2O$, but no tungsten analogue could be obtained.

The X-ray analysis of complex **4** reveals that a minimal change in the nature of the cation (from NMe_4^+ in **2** to NH_4^+ here) results in a dramatic change in the resultant complex (*i.e.* from dinuclear in **2** to mononuclear in **4**), Fig. 4. The molybdenum atom again has pentagonal-bipyramidal geometry with the primary axial site occupied by an oxo ligand and the

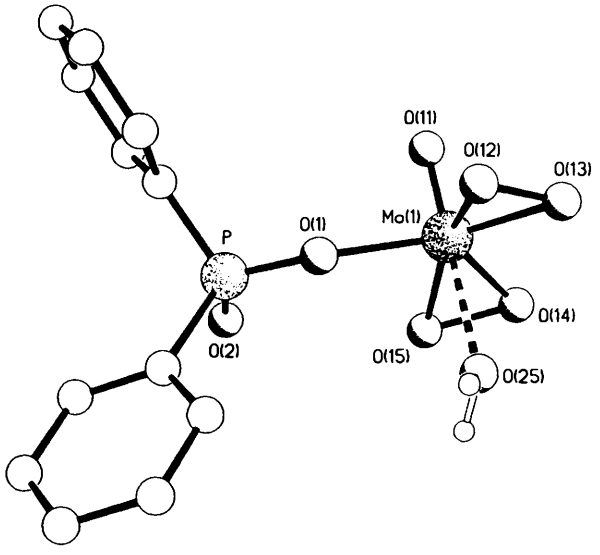

Fig. 4 Structure of the anion in complex **4**

equatorial positions filled by two η^2-peroxo groups and a diphenylphosphinate oxygen atom. The secondary axial position, in the absence of any η^2,η^1 interaction, is occupied by an aqua ligand. The Mo–OH_2 distance of 2.368(2) Å is typical of that observed in other molybdenum and tungsten diperoxo species.[1,15] The overall co-ordination geometry again differs little from that observed in the dinuclear molybdenum and tungsten species **1**, **2** and **3** (see Table 1).

As expected, the P–O(1) distance [1.536(2) Å] is significantly longer than P–O(2) [1.488(2) Å], the latter retaining its double bond character.

An analysis of the packing of the molecules reveals that the NH_4^+ cation plays, together with the aqua ligand, a major role in the determination of the solid-state superstructure. The NH_4^+ cation is almost promiscuous in its nature, distributing its favours equally, forming N–H • • • O hydrogen bonds to phosphinato oxo [O(2)], peroxo [O(13)], aqua [O(25)] and oxo [O(11)] oxygen atoms of adjacent molecules (depicted, by links a, b, c and d respectively, in Fig. 5). One of the hydrogen atoms of the aqua ligand is linked to one of the peroxo oxygen atoms [O(15)] of a centrosymmetrically related anion, whilst the other links to the phosphinato oxo oxygen atom [O(2)] of a lattice-translated anion (in *a*), depicted, by links e and f

Table 2 Vibrational spectroscopic characteristics (cm^{-1})[a] of complexes **1**–**4**

Complex	ν(M=O)	ν(O–O)	$\nu_{asym}(M_2O)$	$\nu_{asym}[M(O)_2]$	$\nu_{sym}[M(O)_2]$
1	975vs	873vs	*b*	590[b]	549s
	978(10)	*870(9)*	*748(3)*	*586(4)*	*556(3)*
2	968vs	872vs	757s	591s	540s
	970(10)	*879(8)*	*752(3)*	*592(4)*	*533(5)*
3	970vs	846vs	736s	578s	539s
	970(10)	*859(9)*	*704(3)*	*578(4)*	*537(5)*
4	962vs	871vs	—	581s	553s
	956(10)	*875(6)*	—	*577(2)*	*538(3)*

[a] Raman data in italics (relative intensities in parentheses). [b] Band obscured by the cacodylate ion.

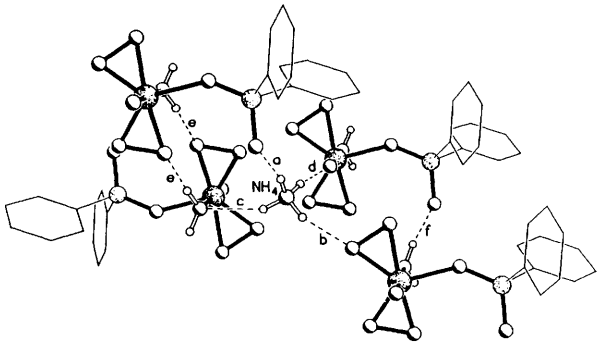

Fig. 5 Part of the extended hydrogen bonding in the structure of complex **4**, showing the environment of the ammonium cation. Hydrogen bonding geometries; N · · · O and H · · · O distances (Å) and N–H · · · O angle (°), a, 2.83, 1.94, 166; b, 2.85, 2.21, 128; c, 2.98, 2.15, 153; d, 3.10, 2.22, 166; O · · · O and H · · · O distances (Å) and O–H · · · O angle (°), e, 2.75, 1.85, 174; f, 2.71, 1.81, 172

respectively, in Fig. 5. The combination of these hydrogen-bonding interactions produces extended sheets, two complexes thick, that extend in the crystallographic *a* and *b* directions.

Vibrational and ^{31}P-{^1H} NMR spectroscopy

The infrared and Raman spectra of complexes **1**–**4** (Table 2) show features comparable to those observed for $[NMe_4]_2[(PhPO_3)\{WO(O_2)_2\}_2\{WO(O_2)_2(H_2O)\}]$[1] and $[(XO_4)\{MO(O_2)_2\}_4]^{3-}$ [M = Mo or W, X = P or As].[2] Bands near 970 cm^{-1} are assigned as ν(M=O), those between 845 and 880 cm^{-1} as ν(O–O) of the η^2-peroxo ligands and those around 580 and 535 cm^{-1} as asymmetric and symmetric $[M(O_2)]$ stretches, respectively. Our assignments are based on those established by us for Venturello's complex.[2] In addition to bands due to the counter ions, NMe_4^+ and $NBu^n_4^+$, and the diphenylphosphinic acid, P=O stretches appear near 1080 cm^{-1}. Bands due to the cacodylate ligand, $[Me_2AsO_2]^-$, obscure the asymmetric (M_2O) and $[M(O_2)]$ stretches.

The ^{31}P-{^1H} NMR spectra of complexes **2** and **3** in CD_3CN show sharp bands at δ 49.3 and 51.9 respectively, the latter with poorly resolved ^{183}W satellites. The solid-state ^{31}P-{^1H} spectrum of **2** shows a sharp peak at δ 48.0, whilst that of **3** shows two peaks at δ 52.7 and 53.9. This splitting probably reflects the disorder found in the crystal structure, but it nevertheless seems likely that **2** and **3** have essentially the same structures in solution as in the solid state. Unfortunately the complexes were not sufficiently soluble to allow the Raman spectra of solutions to be recorded. The solid-state NMR spectrum of **4** shows two sharp peaks at δ 33.2 and 30.5, but unfortunately solution spectra could not be obtained due to the low solubility of the complex.

The NMR spectra of solutions of complexes **2** and **3** in CD_3CN with added H_2O_2 show broad bands at δ 49.1 (**2**) and 46.7 (**3**), and sharp bands at 28.7 (**2**) and 30.1 (**3**). The sharp bands increase in intensity as the concentration of H_2O_2 is increased. It seems likely that for **2** the δ 49.1 band arises from the monoanionic species $[(Ph_2PO_2)\{MoO(O_2)_2\}_2]^-$ and the δ 28.7 band from $[(Ph_2PO_2)\{MoO(O_2)_2(H_2O)\}]^-$, the anion of **4**. If this is so, then the sharp δ 30.1 band of **3** could arise from the otherwise unknown tungsten analogue of the monomer **4**.

Epoxidation of cyclic and linear alkenes

In the presence of the phase-transfer cation $[N(C_6H_{13})_4]Cl$ in a 1 : 1 (cation : complex) ratio (this was found to be the optimum ratio), complex **3** will cleanly catalyse the epoxidation of a number of cyclic and linear alkenes in a biphasic 15% H_2O_2–benzene mixture at 75 °C (Table 3). The epoxidation of small ring cycloalkenes over 3 h is less effectively carried out in comparison with those of larger ring cycloalkenes. The epoxidations are slightly less efficient than those catalysed by either $[N(C_6H_{13})_4]_3[PO_4\{WO(O_2)_2\}_4]$[2] or $[NMe_4]_2[(PhPO_3)\{WO(O_2)_2\}\{WO(O_2)_2(H_2O)\}]$[1] under similar reaction conditions. The oxidation of linear primary alkenes, carried out for 20 h, gave a low yield of epoxide, though the yields were higher for longer chain alkenes. The presence of the phenyl rings clearly has some effect on the catalytic ability as complex **3** is not as efficient as the other dinuclear tungsten complex reported, $[NBu^n_4]_2[\{PO_3(OH)\}\{WO(O_2)_2\}_2]$.[14] Neumann and Miller,[16] however, have recently shown that quaternary ammonium salts of $[PO_4\{WO(O_2)_2\}_4]^{3-}$ can be attached *via* phenyl groups to silica particles. It is therefore of interest to design complexes (as has been done here) in which organo ligands, for example phenyl groups, are bound to the hetero-atom as possible anchor points for attachment of the catalysts to surfaces such as silica.

The molybdenum complexes **1** and **2**, in the presence of a stoichiometric amount of phase-transfer agent, will also catalyse alkene epoxidation, though far less efficiently than **3**. This often appears to be the case with oxidations using molybdenum and tungsten complexes in which H_2O_2 is the cooxidant.[17] The mononuclear complex **4**, which contains only η^2-peroxo groups, is an even poorer catalyst than either **1** or **2** for the epoxidation of cyclic alkenes.

Oxidation of primary and secondary alcohols and tertiary amines

When complex **3** is used as a catalyst for the oxidation of primary and secondary alcohols under the same conditions as described above for the epoxidation of cyclic alkenes, good yields of aldehyde and ketone respectively are obtained (Table 4). As the size of the ring of the secondary cyclic alcohols is increased, the yield of ketone increases. The oxidation of tertiary amines catalysed by **3** was also successfully carried out and good yields of the corresponding *N*-oxides obtained (Table 5); these reactions were typically carried out at 90 °C in a biphasic 15% H_2O_2–toluene mixture for 5 h. Again the molybdenum complexes **1** and **2** are not as efficient as **3** for these transformations. Complex **3** is a better oxidation catalyst than $[NMe_4]_2[(PhPO_3)\{WO(O_2)_2\}\{WO(O_2)_2(H_2O)\}]$ for alcohols in respect of yields though not turnovers, and is

Table 3 Epoxidation of cyclic and linear alkenes by $[NBu^n_4][(Ph_2PO_2)\{WO(O_2)_2\}_2]$ **3***

Substrate	Product	Yield (%) [turnover]
Cyclopentene	Cyclopentene oxide	16 [24]
Cyclohexene	Cyclohexene oxide	8 [12]
Cycloheptene	Cycloheptene oxide	67 [101]
Cyclooctene	Cyclooctene oxide	85 [128]
Cyclododecene	Cyclododecene oxide	30 [45]
Hept-1-ene	1,2-Epoxyheptane	8 [12]
Oct-1-ene	1,2-Epoxyoctane	23 [35]
Non-1-ene	1,2-Epoxynonane	31 [47]
Dec-1-ene	1,2-Epoxydecane	32 [48]
Undec-1-ene	1,2-Epoxyundecane	34 [51]
Dodec-1-ene	1,2-Epoxydodecane	35 [53]

* Reactions were carried out in a benzene–peroxide system refluxing at 75 °C for 3 h for cyclic alkenes and 20 h for linear alkenes.

Table 4 Oxidation of primary and secondary alcohols by $[NBu^n_4][(Ph_2PO_2)\{WO(O_2)_2\}_2]$ **3***

Substrate	Product	Yield (%) [turnover]
Benzyl alcohol	Benzaldehyde	76 [114]
2-Methylbenzyl alcohol	2-Methylbenzaldehyde	76 [114]
4-Methylbenzyl alcohol	4-Methylbenzaldehyde	85 [128]
Cyclopentanol	Cyclopentanone	37 [56]
Cyclohexanol	Cyclohexanone	55 [83]
2-Methylcyclohexanol	2-Methylcyclohexanone	72 [108]
3-Methylcyclohexanol	3-Methylcyclohexanone	63 [95]
4-Methylcyclohexanol	4-Methylcyclohexanone	59 [89]
Cycloheptanol	Cycloheptanone	91 [137]
Cyclooctanol	Cyclooctanone	94 [141]
Menthol	Menthone	53 [80]
1-Phenylethanol	Acetophenone	85 [128]

* Reactions were carried out in a benzene–peroxide system refluxing at 75 °C for 3 h.

comparable in effectiveness for oxidation of tertiary amines with $[N(C_6H_{13})_4]_2[W_2O_3(O_2)_4]$ and $[N(C_6H_{13})_4]_3[XO_4\{WO(O_2)_2\}_4]$ (X = As or P).[6]

Conclusion

In the previous paper in the series[1] we intimated that the presence of η^2,η^1-peroxo groups is a key feature in determining the catalytic oxidation properties of heteropolyperoxo complexes containing an organic phosphonate. Here we have demonstrated this principle to hold for the simpler dinuclear arsinate and phosphinate species **1**–**3**. It is still not clear, however, why the presence or absence of such linkages should have such a marked effect on the catalytic efficacy, though we have discussed possible reasons for this earlier.[1]

Complexes **1**–**4** all have essentially identical distorted pentagonal-bipyramidal geometries with two equatorial peroxo groups, a short axial oxo ligand and a significantly longer *trans* axial M–O bond; the latter arises from an η^2,η^1-peroxo linkage in complexes **1**–**3** and an aqua ligand in **4**.

Experimental

X-Ray crystallography

A summary of the crystal data, data collection and refinement parameters for compounds **1**–**4** is given in Table 6. All four structures were solved by direct methods and the major occupancy non-hydrogen atoms were refined anisotropically. In **3**, the minor occupancy (45%) oxygen atoms were refined isotropically. In **4**, both phenyl rings were found to have well defined, alternative, 50% partial occupancy orientations, all of which were refined anisotropically. The phenyl rings in structures **2**–**4** were refined as optimised rigid bodies. All C–H hydrogen atoms were placed in idealised positions, assigned isotropic thermal parameters, $U(H) = 1.2U_{eq}(C)$ [$U(H) = 1.5U_{eq}$(C–Me)] and allowed to ride on their parent carbon atoms. In **4**, the positions of the ammonium and aqua hydrogen atoms were determined from a ΔF map and refined isotropically subject to N–H and O–H distance constraints (0.90 Å). Refinement in all cases was by full-matrix least squares based on F^2. Computations were carried out on 50 MHz 486DX PC computers using the SHELXTL PC program system.[18]

Atomic coordinates, thermal parameters and bond lengths and angles have been deposited at the Cambridge Crystallographic Data Centre (CCDC). See Instructions for Authors, 1996, Issue 1. Any request to the CCDC for this material should quote the full literature citation and the reference number 186/9.

Table 5 Oxidation of tertiary amines by $[NBu^n_4][(Ph_2PO_2)\{WO(O_2)_2\}_2]$ **3***

Substrate	Yield of *N*-oxide (%) [turnover]
Pyridine-2-carboxylic acid	58 [87]
Nicotinic acid	72 [108]
Isonicotinic acid	57 [86]
Pyridine-2,3-dicarboxylic acid	71 [107]
Pyridine-2,5-dicarboxylic acid	27 [41]
Pyridine-2,6-dicarboxylic acid	86 [129]
Pyridine-3,4-dicarboxylic acid	85 [128]

* Reactions were carried out in a toluene–peroxide system refluxing at 90 °C for 5 h.

General

Infrared spectra of the solids were measured over the range 4000–400 cm^{-1} using KBr discs on a Perkin-Elmer 1720 Fourier-transform spectrometer, Raman spectra of the solids (as powders in melting-point tubes) on a Perkin-Elmer 1760X FT-IR instrument fitted with a 1700X NIR FT-Raman accessory using a Nd:YAG laser (1064 nm excitation). The NMR spectra were obtained on a JEOL ESX 270 spectrometer (^{31}P, 109.25 MHz) as CD_3CN solutions, using external H_3PO_4 as reference. The gas chromatography data were obtained on a Perkin-Elmer Autosystem instrument using a Perkin-Elmer stainless steel column (2 m) packed with 5% Carbowax 20M on Chromasorb WHP AW (DCMS treated). Microanalyses were carried out by the Microanalytical Laboratories at Imperial College.

The trioxides $MoO_3{\cdot}H_2O$ and $WO_3{\cdot}H_2O$ were obtained from BDH and Fluka Chemie AG, respectively. Hydrogen peroxide was obtained from BDH as a 30% w/v aqueous solution and was used as supplied. Diphenylphosphinic acid and cacodylic acid (dimethylarsinic acid) were both obtained from Aldrich.

Syntheses

$[NMe_4][(Me_2AsO_2)\{MoO(O_2)_2\}_2]$ 1. Hydrated molybdenum trioxide, $MoO_3{\cdot}H_2O$ (0.72 g, 5.0 mmol), was suspended in aqueous hydrogen peroxide solution (4 cm^3, 30% w/v) and the resulting suspension stirred at 30 °C until a yellow solution was obtained. Upon cooling to ambient temperature, Na-$[Me_2AsO_2]$ (0.40 g, 2.5 mmol) in ethanol (5 cm^3) was added followed by dropwise addition of $[NMe_4]Cl$ (0.27 g, 2.5 mmol) in water (5 cm^3). Ethanol (5 cm^3) was added and the mixture cooled to 4 °C. The bright yellow crystalline solid was filtered off, washed with cold ethanol (2 × 5 cm^3) and diethyl ether (10 cm^3) and then air dried. Yield 1.2 g, 2.13 mmol (85%) (Found: C, 12.8; H, 2.9; N, 2.5. Calc. for $C_6H_{18}AsMo_2NO_{12}$: C, 12.8; H, 3.2; N, 2.5%).

Table 6 Crystallographic data for complexes **1–4**[a]

	1	**2**	**3**	**4**
Chemical formula	$C_6H_{18}AsMo_2NO_{12}$	$C_{16}H_{22}Mo_2NO_{12}P$	$C_{28}H_{46}NO_{12}PW_2$	$C_{12}H_{16}MoNO_8P$
M	563.01	643.20	987.33	429.2
Crystal system	Monoclinic	Monoclinic	Triclinic	Triclinic
Space group	$P2_1/c$	$P2_1/n$	$P\bar{1}$	$P\bar{1}$
a/Å	14.098(1)	11.203(1)	10.352(3)	6.014(1)
b/Å	10.318(1)	18.023(2)	12.776(1)	8.671(2)
c/Å	12.652(2)	11.419(1)	13.641(2)	15.328(3)
α/°			98.069(9)	87.90(2)
β/°	113.324(7)	97.095(6)	100.89(2)	86.92(2)
γ/°			91.77(1)	86.56(2)
U/Å^3	1690.0(3)	2288.1(4)	1751.1(6)	796.3(3)
Z	4	4	2	2
D_c/g cm^{-3}	2.213	1.867	1.873	1.790
μ/mm^{-1}	3.482	1.227	6.667	0.964
F(000)	1096	1280	960	432
Colour, habit	Yellow, blocks	Yellow, blocks	Clear, prisms	Yellow, blocks
Crystal size/mm	0.92 × 0.48 × 0.23	0.80 × 0.37 × 0.23	0.27 × 0.22 × 0.13	0.59 × 0.40 × 0.28
2θ Range/°	5–50	4–50	4–50	7–50
Independent reflections (R_{int})	2955 (0.02)	4046 (0.02)	5578 (0.03)	2788 (0.02)
Observed reflections [$\|F_o\| > 4\sigma(\|F_o\|)$]	2587	3628	3272	2612
Absorption correction	Empirical	Semi-empirical	Semi-empirical	
Maximum, minimum transmission	0.7736, 0.2883	0.4543, 0.3993	0.6631, 0.3598	
No. of parameters	199	266	414	292
a, b in weighting scheme[b]	0.0819, 1.5095	0.0365, 1.8123	0.0457, 10.8730	0.0388, 0.7700
Final R_1 (wR_2)[c]	0.044 (0.115)	0.028 (0.072)	0.060 (0.122)	0.026 (0.071)
Largest, mean Δ/σ	−0.001, 0.000	−0.001, 0.000	0.542, 0.047	−0.006, 0.001
Data : parameter ratio	13.0	13.6	7.90	8.95
Largest difference peak, hole/e Å^{-3}	0.89, −0.87	0.37, −0.41	1.13, −1.54	0.43, −0.38

[a] Details in common: Siemens P4/PC diffractometer, graphite-monochromated Mo-Kα radiation, ω scans, room temperature, data corrected for Lorentz and polarisation factors, refinement based on F^2. [b] $w^{-1} = \sigma^2(F_o^2) + (aP)^2 + bP$. [c] $wR_2 = \{\Sigma[w(F_o^2 - F_c^2)^2]/\Sigma[w(F_o^2)^2]\}^{\frac{1}{2}}$.

[NBu$^n_4$][(Me$_2$AsO$_2$){MoO(O$_2$)$_2$}$_2$]. Hydrated molybdenum trioxide, $MoO_3 \cdot H_2O$ (0.72 g, 5.0 mmol), was suspended in aqueous hydrogen peroxide solution (4 cm^3, 30% w/v) and the resulting suspension stirred at 30 °C until a yellow solution was obtained. Upon cooling to ambient temperature, Na[Me_2AsO_2] (0.40 g, 2.5 mmol) in ethanol (5 cm^3) was added followed by dropwise addition of [NBu$^n_4$]Cl (0.69 g, 2.5 mmol) in water (5 cm^3). Ethanol (5 cm^3) was added and the mixture cooled to 4 °C. The bright yellow crystalline solid was filtered off, washed with cold ethanol (2 × 5 cm^3) and diethyl ether (10 cm^3) and then air dried. Yield 1.1 g, 1.50 mmol (60%) (Found: C, 30.8; H, 5.5; N, 2.0. Calc. for $C_{18}H_{42}AsMo_2NO_{12}$: C, 29.7; H, 5.8; N, 1.9%).

[NMe$_4$][(Ph$_2$PO$_2$){MoO(O$_2$)$_2$}$_2$] 2. Hydrated molybdenum trioxide, $MoO_3 \cdot H_2O$ (0.72 g, 5.0 mmol), was suspended in aqueous hydrogen peroxide solution (4 cm^3, 30% w/v) and the resulting suspension stirred at 30 °C until a yellow solution was obtained. Upon cooling to ambient temperature, $Ph_2PO(OH)$ (0.55 g, 2.5 mmol) in ethanol (5 cm^3) was added followed by dropwise addition of [NMe_4]Cl (0.27 g, 2.5 mmol) in water (5 cm^3). Ethanol (5 cm^3) was added and the mixture cooled to 4 °C. The bright yellow crystalline solid was filtered off, washed with cold ethanol (2 × 5 cm^3) and diethyl ether (10 cm^3) and air dried. Yield 1.1 g, 1.63 mmol (65%) (Found: C, 29.8; H, 3.1; N, 2.2. Calc. for $C_{16}H_{22}Mo_2NO_{12}P$: C, 29.9; H, 3.5; N, 2.2%).

[NBu$^n_4$][(Ph$_2$PO$_2$){MoO(O$_2$)$_2$}$_2$]. Hydrated molybdenum trioxide, $MoO_3 \cdot H_2O$ (0.72 g, 5.0 mmol), was suspended in aqueous hydrogen peroxide solution (4 cm^3, 30% w/v) and the resulting suspension stirred at 30 °C until a yellow solution was obtained. Upon cooling to ambient temperature, $Ph_2PO(OH)$ (0.55 g, 2.5 mmol) in ethanol (5 cm^3) was added followed by dropwise addition of [NBu$^n_4$]Cl (0.69 g, 2.5 mmol) in water (5 cm^3). Ethanol (5 cm^3) was added and the mixture cooled to 4 °C. The bright yellow crystalline solid was filtered off, washed with cold ethanol (2 × 5 cm^3) and diethyl ether (10 cm^3) and air dried. Yield 1.27 g, 1.56 mmol (62%) (Found: C, 41.5; H, 5.3; N, 1.7. Calc. for $C_{28}H_{46}Mo_2NO_{12}P$: C, 41.4; H, 5.7; N, 1.7%).

[NBu$^n_4$][(Ph$_2$PO$_2$){WO(O$_2$)$_2$}$_2$] 3. Hydrated tungsten trioxide, $WO_3 \cdot H_2O$ (1.25 g, 5.0 mmol), was suspended in aqueous hydrogen peroxide solution (4 cm^3, 30% w/v) and the resulting suspension stirred at 30 °C until a colourless solution was obtained. The resulting solution was centrifuged to remove any insoluble material. Diphenylphosphinic acid (0.55 g, 2.5 mmol) in ethanol (5 cm^3) was added followed by dropwise addition of [NBu$^n_4$]Cl (0.69 g, 2.5 mmol) in water (5 cm^3). Ethanol (5 cm^3) was added and the mixture cooled to 4 °C. The colourless crystalline solid was filtered off, washed with cold ethanol (2 × 5 cm^3) and diethyl ether (10 cm^3) and air dried. Yield 1.9 g, 2.22 mmol (89%) (Found: C, 34.4; H, 4.5; N, 1.4. Calc. for $C_{28}H_{46}NO_{12}PW_2$: C, 34.1; H, 4.7; N, 1.4%).

[NH$_4$][(Ph$_2$PO$_2$){MoO(O$_2$)$_2$(H$_2$O)}] 4. Hydrated molybdenum trioxide, $MoO_3 \cdot H_2O$ (0.72 g, 5.0 mmol), was suspended in aqueous hydrogen peroxide solution (4 cm^3, 30% w/v) and the resulting suspension stirred at 30 °C until a yellow solution was obtained. Upon cooling to ambient temperature $Ph_2PO(OH)$ (1.09 g, 5.0 mmol) in ethanol (5 cm^3) was added followed by dropwise addition of NH_4Cl (0.13 g, 5.0 mmol) in water (5 cm^3). Ethanol (5 cm^3) was added and the mixture cooled to 4 °C. The bright yellow crystalline solid was filtered off, washed with cold ethanol (2 × 5 cm^3) and diethyl ether (10 cm^3) and air dried. Yield 1.6 g, 3.73 mmol (75%) (Found: C, 33.4; H, 3.7; N, 3.3. Calc. for $C_{12}H_{16}MoNO_8P$: C, 33.6; H, 3.8; N, 3.3%).

General procedure for epoxidation of cycloalkenes

The catalyst **3** (0.1 mmol) and [$N(C_6H_{13})_4$]Cl (0.1 mmol) were dissolved in benzene (8 cm^3) and the alkene (15 mmol) added. Hydrogen peroxide (15% w/v, 10 cm^3) was added to the

benzene solution and the biphasic mixture refluxed at 75 °C for 3 h. The resulting organic layer was then analysed by gas chromatography.

General procedure for epoxidation of linear alkenes

The catalyst **3** (0.1 mmol) and $[N(C_6H_{13})_4]Cl$ (0.1 mmol) were dissolved in benzene (8 cm^3) and the alkene (15 mmol) added. Hydrogen peroxide (15% w/v, 10 cm^3) was added to the benzene solution and the biphasic mixture refluxed at 75 °C for 20 h. The resulting organic layer was then analysed by gas chromatography and/or ^1H NMR spectroscopy.

General procedure for oxidation of primary and secondary alcohols

The catalyst **3** (0.1 mmol) and $[N(C_6H_{13})_4]Cl$ (0.1 mmol) were dissolved in benzene (8 cm^3) and the alkene (15 mmol) added. Hydrogen peroxide (15% w/v, 10 cm^3) was added to the benzene solution and the biphasic mixture refluxed at 75 °C for 3 h. The resulting organic layer was then analysed by gas chromatography.

General procedure for oxidation of tertiary amines

The catalyst **3** (0.1 mmol) and $[N(C_6H_{13})_4]Cl$ (0.1 mmol) were dissolved in toluene (8 cm^3) and the alkene (15 mmol) added. Hydrogen peroxide (15% w/v, 10 cm^3) was added to the toluene solution and the biphasic mixture refluxed at 90 °C for 5 h. Upon cooling the solid was filtered off, washed with water (5 cm^3), diethyl ether (2 × 10 cm^3) and air dried. The yield, IR spectrum and melting point of the product were recorded.

Acknowledgements

We thank the EPSRC for a postdoctoral fellowship to one of us (B. C. P.) and Solvay-Interox and the EPSRC for a CASE award to N. M. G. The University of London Intercollegiate Research Service is thanked for the Raman spectrometer and the EPSRC for the X-ray diffractometer. We thank Patrick Barrie and David Butler of the University of London Intercollegiate Research Service for running the solid-state NMR spectra, and Bill Sanderson and Craig Jones of Solvay-Interox, Widnes for helpful discussions.

References

1 W. P. Griffith, B. C. Parkin, A. J. P. White and D. J. Williams, *J. Chem. Soc., Dalton Trans.*, 1995, 3131.
2 A. C. Dengel, W. P. Griffith and B. C. Parkin, *J. Chem. Soc., Dalton Trans.*, 1993, 2683.
3 C. Venturello, R. D'Aloisio, J. C. Bart and M. Ricci, *J. Mol. Catal.*, 1985, **32**, 107.
4 W. P. Griffith, B. C. Parkin, A. J. P. White and D. J. Williams, *J. Chem. Soc., Chem. Commun.*, 1995, 2183; L. Salles, C. Aubry, F. Robert, G. Chottard, R. Thouvenot, H. Ledon and J.-M. Brégeault, *New J. Chem.*, 1993, **17**, 367; C. Aubry, G. Chottard, N. Platzer, J.-M. Brégeault, R. Thouvenot, F. Chauveau, C. Huet and H. Ledon, *Inorg. Chem.*, 1991, **30**, 4409; C. Venturello and M. Gambaro, *Synthesis*, 1989, **4**, 295; C. Venturello and R. D'Aloisio, *J. Org. Chem.*, 1988, **53**, 1553.
5 D. C. Duncan, R. C. Chambers, E. Hecht and C. L. Hill, *J. Am. Chem. Soc.*, 1995, **117**, 681.
6 A. J. Bailey, W. P. Griffith and B. C. Parkin, *J. Chem. Soc., Dalton Trans.*, 1995, 1833.
7 Y. Ishii and Y. Sakato, *J. Org. Chem.*, 1990, **55**, 5545.
8 Y. Ishii and Y. Sakato, *Studies in Surface Science and Catalysis*, ed. L. I. Simandi, Elsevier, Amsterdam, 1991, vol. 66, p. 411.
9 S. Sakaguchi, S. Watase, Y. Katayama, Y. Nishiyama and Y. Ishii, *J. Org. Chem.*, 1994, **59**, 5681.
10 Y. Ishii, K. Yamawaki, Y. Ura, H. Yamada, T. Yoshida and M. Ogawa, *J. Org. Chem.*, 1988, **53**, 3587.
11 S. Sakaue, T. Sakata, Y. Nashiyama and Y. Ishii, *Chem. Lett.*, 1992, 289.
12 S. Sakaue, T. Tsubakino, Y. Nishiyama and Y. Ishii, *J. Org. Chem.*, 1993, **58**, 3633.
13 Y. Ishii, H. Tanaka and Y. Nishiyama, *Chem. Lett.*, 1994, 1.
14 L. Salles, C. Aubry, R. Thouvenot, F. Robert, C. Dorémieux-Morin, G. Chottard, H. Ledon, V. Jeannin and J.-M. Brégeault, *Inorg. Chem.*, 1994, **33**, 871.
15 F. W. B. Einstein and B. R. Penfold, *Acta Crystallogr.*, 1964, **17**, 1127.
16 R. Neumann and H. Miller, *J. Chem. Soc., Chem. Commun.*, 1995, 2277.
17 G. Amato, A. Arcoria, F. P. Ballistreri, G. A. Tomaselli, O. Bortolini, C. Conte, F. di Furia, G. Modena and G. Valle, *J. Mol. Catal.*, 1986, **37**, 165.
18 SHELXTL PC, Release 5.03, Siemens Analytical X-Ray Instruments Inc., Madison, WI, 1994.

Received 15*th December* 1995; *Paper* 5/08161K